

Incipient Melting in AA7075

SAND20XX-XXXX

Printed June 2022



Sandia
National
Laboratories

Incipient Melting in AA7075

Johnathon Brehm, Jessica Buckner, Christina Profazi, Alex Hickman

Prepared by
Sandia National Laboratories
Albuquerque, New Mexico
87185 and Livermore,
California 94550

Issued by Sandia National Laboratories, operated for the United States Department of Energy by National Technology & Engineering Solutions of Sandia, LLC.

NOTICE: This report was prepared as an account of work sponsored by an agency of the United States Government. Neither the United States Government, nor any agency thereof, nor any of their employees, nor any of their contractors, subcontractors, or their employees, make any warranty, express or implied, or assume any legal liability or responsibility for the accuracy, completeness, or usefulness of any information, apparatus, product, or process disclosed, or represent that its use would not infringe privately owned rights. Reference herein to any specific commercial product, process, or service by trade name, trademark, manufacturer, or otherwise, does not necessarily constitute or imply its endorsement, recommendation, or favoring by the United States Government, any agency thereof, or any of their contractors or subcontractors. The views and opinions expressed herein do not necessarily state or reflect those of the United States Government, any agency thereof, or any of their contractors.

Printed in the United States of America. This report has been reproduced directly from the best available copy.

Available to DOE and DOE contractors from

U.S. Department of Energy
Office of Scientific and Technical Information
P.O. Box 62
Oak Ridge, TN 37831

Telephone: (865) 576-8401
Facsimile: (865) 576-5728
E-Mail: reports@osti.gov
Online ordering: <http://www.osti.gov/scitech>

Available to the public from

U.S. Department of Commerce
National Technical Information Service
5301 Shawnee Rd
Alexandria, VA 22312

Telephone: (800) 553-6847
Facsimile: (703) 605-6900
E-Mail: orders@ntis.gov
Online order: <https://classic.ntis.gov/help/order-methods/>



ABSTRACT

Incipient melting is a phenomenon that can occur in aluminum alloys where solute rich areas, such as grain boundaries, can melt before the rest of the material; incipient melting can degrade mechanical and corrosion properties and is irreversible, resulting in material scrapping. After detecting indications of incipient melting as the cause of failure in 7075 aluminum alloy parts (AA7075), a study was launched to determine threshold temperature for incipient melting. Samples of AA7075 were solution annealed using temperatures ranging from 870-1090°F. A hardness profile was developed to demonstrate the loss of mechanical properties through the progression of incipient melting. Additionally, Zeiss software Zen Core Intellesis was utilized to more accurately quantify the changes in microstructural properties as AA7075 surpassed the onset of incipient melting. The results from this study were compared with previous AA7075 material that demonstrated incipient melting.

CONTENTS

Abstract.....	3
Executive Summary.....	7
Acronyms and Terms	8
1. Background	9
1.1. Basics.....	9
1.2. Previous Cases of Incipient Melting	12
2. Experimental Set-Up	13
2.1. Starting Material	13
2.2. Heat Treatment.....	13
2.3. Metallographic Analysis	14
3. Hypothesis.....	15
4. Results.....	16
4.1. Optical Microscopy	16
4.1.1. Temperature-Dependent Data	16
4.1.2. Time-Dependent Data.....	18
4.2. Electron Dispersive Spectroscopy	21
4.3. Zeiss Intellesis Image Analysis.....	23
4.3.1. Temperature-Dependent Data	23
4.3.2. Time-Dependent Data.....	26
4.4. Vickers Micro-Indentation	28
4.4.1. Temperature-Dependent Data	28
4.4.2. Time-Dependent Data.....	28
References	30
Distribution.....	31

LIST OF FIGURES

Figure 1. Representative AA7075 microstructure after solution anneal, as-polished condition	10
Figure 2. Al-Zn binary phase diagram.....	11
Figure 3. As-polished micrographs of 'Case A' incipient melting.....	12
Figure 4. Temperature-dependent micrographs	17
Figure 5. Time-dependent micrographs	19
Figure 6. Extent of cracking in time-dependent samples	20
Figure 7. EDS map of 1090°F sample.....	22
Figure 8. Trends in the Zeiss Intellesis data for temperature-dependence.....	24
Figure 9. Temperature-dependent Zeiss Intellesis image analysis results	25
Figure 10. Trends in the Zeiss Intellesis data for time-dependence	26
Figure 11. Time-dependent Zeiss Intellesis image analysis results	27
Figure 12. Temperature-dependent hardness data	28
Figure 13. Time-dependent hardness data.....	29

LIST OF TABLES

Table 1. Standard Chemistry Range for AA7075, based on ASTM B221	10
Table 2. Comparison of mechanical properties between the study material and ASTM B221	11
Table 3. AA7075 study material composition	13
Table 4. Solution anneal temperature/time matrix	14
Table 5. Hypothesized liklihood of incipient melting occurring based on temperature/time	15
Table 6. Hypothesized results for microstructural features and hardness properties	15
Table 7. Zeiss Intellesis image analysis results for temperature-dependence	23
Table 8. Zeiss Intellesis image analysis results for time-dependence	26

This page left blank

EXECUTIVE SUMMARY

Several instances of incipient melting have recently been detected in forged AA7075, resulting in part failures and high scrap rates. Considering the industrial processing that AA7075 undergoes, there are three variables that may contribute to incipient melting: strain from forging, temperature, and time at a certain temperature. This experiment focused on the solution anneal process and evaluated the effects that both temperature and time have on the properties of AA7075. These results were compared to previous material ‘Case A’ where incipient melting was detected. Since strain from forging was not considered, the onset of incipient melting observed in this study most likely occurred at higher temperatures than what would occur in practice.

The temperature-dependent optical results revealed that the first signs of incipient melting were detected at 925°F, when the agglomeration of Al₂CuMg particles was first detected. However, more obvious signs of incipient melting didn’t occur until 1035°F, when triple points and eutectic phase networked along the grain boundaries. The time-dependent optical results revealed that extended times at a certain temperature increased the amount of cracking and triple-points but had no other affect. When considering temperature and time in this experiment, temperature was much more impactful in contributing to incipient melting.

The temperature-dependent hardness results exhibited no noticeable decrease in hardness until 1090°F. Due to this, hardness testing is not recommended when trying to detect incipient melting in AA7075, as the lowest temperature that a change in hardness was detected (1090°F) was 165°F above the temperature where the first signs of incipient melting were seen using optical microscopy (925°F). The time-dependent study demonstrated that solution anneal hold time does not impact the hardness of AA7075.

Zeiss Intellesis image analysis revealed several relationships in the data. A positive correlation was detected between temperature and triple-points from 980°F to 1090°F. A positive correlation was detected between temperature and eutectic phase 980°F to 1090°F. Additionally, a positive correlation between hold time and triple-points was detected from a 1-hour hold time to a 24-hour hold time.

Comparing the study results to a previous case of incipient melting ‘Case A’, there are similarities between the ‘Case A’ material and the 1035°F sample. Both exhibited signs of triple-points and increased agglomeration of Al₂CuMg. However, one significant difference was that the 1035°F sample demonstrated a network of eutectic phase along the grain boundaries, while the ‘Case A’ material did not. This difference most likely can be attributed to the fact that the ‘Case A’ material also experienced a forging process, where the strain from forging helped initiate incipient melting at a lower temperature where triple-points formed yet eutectic phase didn’t.

ACRONYMS AND TERMS

Acronym/Term	Definition
AA7075	7075 aluminum alloy
SEM	Scanning electron microscopy
EDS	Electron dispersive spectroscopy
ICP	Inductively coupled plasma

1. BACKGROUND

1.1. Basics

7xxx-series, or aluminum-zinc alloys, are heat-treatable and are alloyed primarily with zinc but also have appreciable amounts of magnesium, copper, chromium, and iron. Desirable properties, such as high strength, corrosion resistance and a lower risk of fatigue crack growth are reasons why this alloy class is commonly used in aerospace and automobile applications. 7075 aluminum alloy (AA7075) is a popular alloy with the 7xxx-series of aluminum which features slightly higher quantities of chromium and magnesium than similar alloys within its class [3]. A standard chemistry for AA7075 can be found in Table 1. The increased addition of chromium helps give a slight boost to strength and aids in preventing recrystallization during heat treatment. Elevating the magnesium levels helps give a further boost of strength in AA7075 [3]. Typical mechanical properties for this alloy according to ASTM B221 are listed in Table 2.

To obtain desirable mechanical properties, the AA7075 that is processed for Sandia National Laboratories typically undergoes the following forming process and heat treatment [1].

- Forge: shaping the material by heating it and applying pressure preferentially.
- Solution Anneal: dissolves precipitates into solution
- Quench: submerging the material in water (140°F – 160°F) to quickly cool the material and trap the precipitates in solution [1]
- Age: brings strengthening precipitates back out of solution

Typically, the primary strengthening precipitate in AA7075 is MgZn₂. Other phases frequently present include Al₇Cu₂Fe and Al₂CuMg. Al₇Cu₂Fe is an insoluble iron-bearing phase that appears darker than other constituents in the as-polished condition and can appear ‘jagged’ with sharp edges (Fig. 1). Al₂CuMg is a common phase that forms from MgZn₂, and even after a solution anneal, there are appreciable amounts of Al₂CuMg left in the microstructure [4, 5].

If exposed to high enough temperatures for an adequate amount of time, AA7075 starts to undergo several changes. Initially, an increased amount of Al₂CuMg forms from MgZn₂ and begins to agglomerate. As the Al₂CuMg agglomerates, it starts to pull MgZn₂ out of solution, leaving behind a low melting eutectic. This low melting eutectic manifests itself as a lamellar-phase that is adjacent to the Al₂CuMg and represents alloy-depleted areas known as rosettes (Fig. 1). Rosettes are often circular and serve as the harbinger of incipient melting. Incipient melting is melting that occurs below the bulk melting temperature due to localized segregation. As the temperature increases further, rosettes increasingly appear along grain boundaries and can merge to create large-scale grain boundary melting given the right conditions (usually a combination of temperature, time, and strain). Triple-points and intergranular cracking are typically observed at this point. When these phenomena (incipient melting, cracking, etc.) are present in aluminum, it is a sign that mechanical properties have deteriorated to the point where the material must be scrapped [4,5].

Table 1. Standard Chemistry Range for AA7075, based on ASTM B221

Standard Chemistry	Weight % Range
Fe	0 - 0.5
Cu	1.2 – 2.0
Mg	2.1 - 2.9
Cr	0.18 - 0.28
Zn	5.1 - 6.1
Al	Remainder

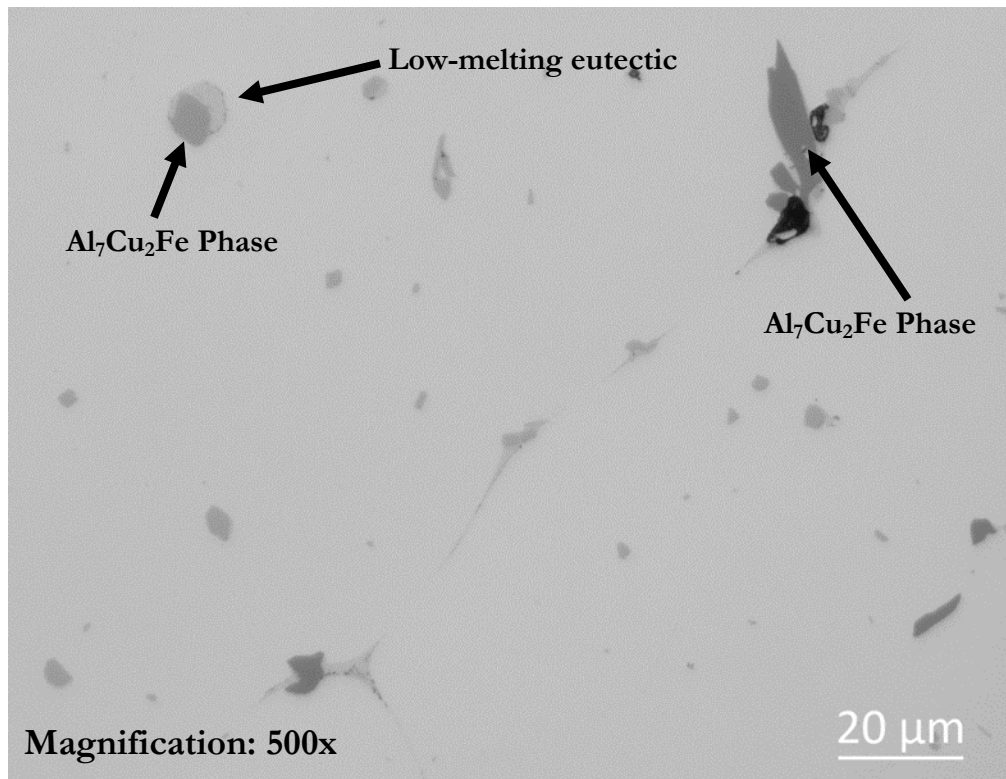
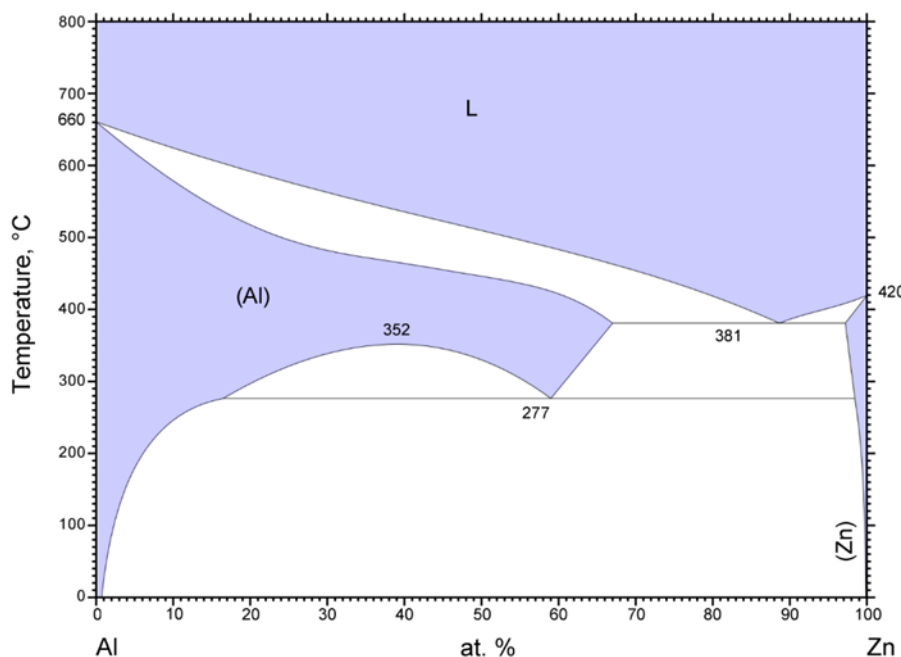


Figure 1. Representative AA7075 microstructure after solution anneal, as-polished condition

Table 2. Comparison of mechanical properties between the study material and ASTM B221

	ASTM B221	Study Material
Ultimate Tensile Strength	81,000 psi	83,200 psi
Tensile Yield Strength	72,000 psi	75,800 psi
Elongation	7%	16.5%

This AA7075 material typically undergoes forging, followed by a heat treatment featuring a solution anneal, quench, and aging process. The standard heat treatment for this alloy, according to the AMS 2770 Rev. P specification, includes an 870°F solution anneal followed by a quench [1]. AA7075 is unique in the fact that the recommended solution anneal temperature (870°F) is extremely close to its theoretical incipient melting temperature (905°F-910°F). Because of this, incipient melting and subsequent loss of mechanical properties is unfortunately a common occurrence. In fact, several instances of incipient melting have recently been detected in forged AA7075, resulting in part failures and high scrap rates. One instance of this is documented in Section 1.2. Considering the industrial processing that AA7075 undergoes, there are three variables that may contribute to incipient melting: strain from forging, temperature, and time at a certain temperature. This experiment focused on the solution anneal process and evaluated the effects that both temperature and time have on the properties of AA7075. These results were also compared to previous material where incipient melting was detected. Since strain from forging was not considered, the onset of incipient melting observed in this study most likely occurred at higher temperatures and longer times than what would occur in practice.



© ASM International 2007. Diagram No. 100056

Figure 2. Al-Zn binary phase diagram [6]

1.2. Previous Cases of Incipient Melting

This section aims to showcase a previously documented case of incipient melting in AA7075 and serve as a comparison to the data obtained in this study. For the purposes of this report, this case will be referred to as 'Case A'. The material associated with Case A didn't demonstrate any signs of incipient melting until a substantial amount of processing had already occurred. 'Case A' underwent forging, machining, solution annealing, and aging before cracking was visible. The troublesome aspect of this is that this material even passed an ultrasonic inspection during its processing, which is a step that is included specifically to catch phenomena such as cracking from incipient melting.

Figure 3 depicts the as-polished microstructure of 'Case A' material and shows evidence of triple-points along the grain boundaries along with signs of Al_2CuMg agglomeration. These are clear signs that incipient melting has affected 'Case A' material. It is worth noting that the 'Case A' material was processed as 7075-T73, while the study material was processed as 7075-T651. This difference in processing parameters was eliminated once the study material underwent its solution anneal.

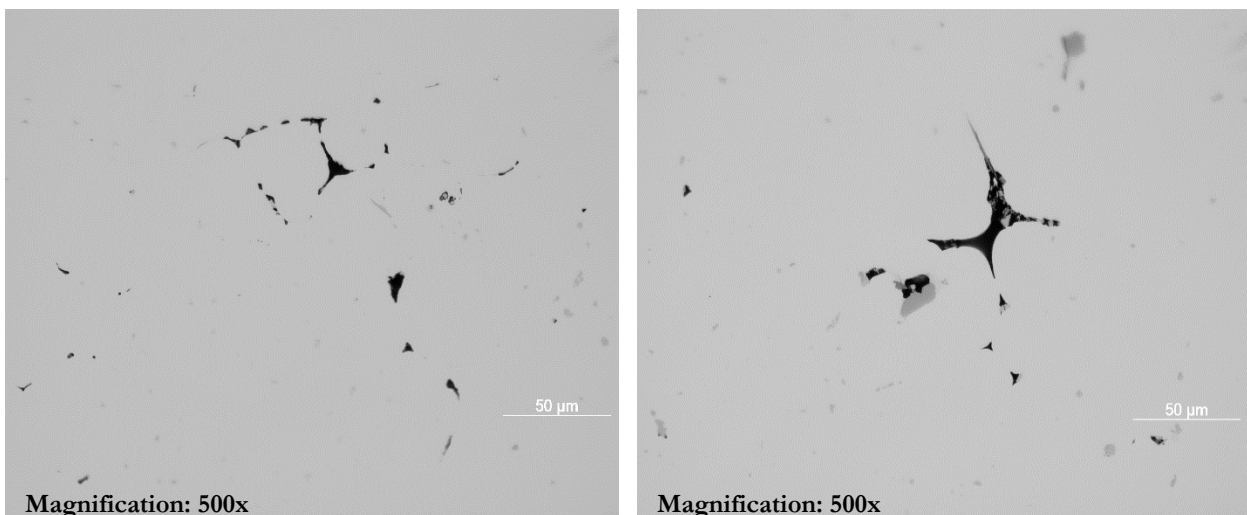


Figure 3. As-polished micrographs of 'Case A' incipient melting

2. EXPERIMENTAL SET-UP

2.1. Starting Material

Two types of experiments were designed to investigate the creation and propagation of incipient melting in AA7075. One experiment titled, ‘Temperature-Dependency’ focused on how changes in solutionizing temperature affect incipient melting. The other experiment, titled ‘Time-Dependency’ focused on how changes in solution annealing time affect incipient melting. For both types of experiments, the same study material was used. This study material was confirmed to be AA7075 using inductively coupled plasma (ICP) and has a composition of that listed in Table 3.

Table 3. AA7075 study material composition

Alloy Element	Actual Weight %	ASTM B221 Weight % Range
Fe	0.13%	0 - 0.5%
Cu	1.39%	1.2 – 2.0%
Mg	2.22%	2.1 - 2.9%
Cr	0.21%	0.18 - 0.28%
Zn	5.4%	5.1 - 6.1%
Al	Remainder	Remainder

2.2. Heat Treatment

The industry standard solution anneal temperature per AMS 2770 Rev. P is 870°F and was defined as the baseline [1]. To induce incipient melting, the temperature was increased in 55°F increments from the baseline, per the heat treatment matrix shown in Table 4. Furnace hold time was held constant at 1 hour for each sample, and the standard quenching procedure per AMS 2770 Rev. P was utilized [1].

The purpose of the time-dependency component of the study was to see if signs of incipient melting at a given temperature were exacerbated with an increase in furnace hold time. Ideally, the temperature used would be the temperature where the first clear-cut signs of large-scale incipient melting occurred in the temperature-dependency aspect of the study. For this reason, the time-dependency component of the study was performed after the completion of the temperature-dependency component. As will be discussed further in Section 4.1, the first signs of large-scale incipient melting occurred at 1035°F, and thus this temperature was chosen for the time-dependency component.

Table 4. Solution Anneal Temperature/Time Matrix

Temperature	Time			
		1 hr	12 hrs	24 hrs
870°F	x			
925°F	x			
980°F	x			
1035°F	x	x		x
1090°F	x			

2.3. Metallographic Analysis

Both types of experiments were analyzed with the same methods. Optical microscopy, primarily done in the as-polished condition, was performed to identify phases and document the appearance and extent of incipient melting. 500gf Vickers micro-indentation hardness testing was done to give a representation of the degradation of mechanical properties as incipient melting progresses. Five Vickers indentations were placed on each sample condition and averaged to obtain representative hardness results. Scanning electron microscopy (SEM), specifically electron dispersive spectroscopy (EDS), was used to help identify phases throughout several solution anneal conditions.

Zeiss Intellesis image analysis software was used to create an image analysis process that analyzed the microstructural features of AA7075 with incipient melting present. This software uses machine learning and can be taught to recognize microstructural features. In this instance, the Zeiss Intellesis software helped quantify the area percentage of microstructural features throughout the incipient melting process, including triple points, lamellar phase, Al₂CuMg, and Al₇Cu₂Fe. There is no Zeiss Intellesis data associated with previous cases of incipient melting, so no comparison was made between 'Case A' and the study material. However, this study aimed to provide foundational data with which future comparison can be made in cases of incipient melting in AA7075. One randomly selected 500x magnification image was used per temperature condition due to time constraints. Further iterations of Zeiss Intellesis image analysis using more temperature and hold time conditions as well as sampling larger surface areas are recommended for future investigation.

3. HYPOTHESIS

Based on the AA7075 phase diagram and literature research, it can reasonably be expected that incipient melting's onset will occur at approximately 910-930°F. The onset of incipient melting is expected to occur with rosettes and the agglomeration of the Al_2CuMg phase. As the extent of incipient melting increases, alloying elements will accumulate along the grain boundaries, causing phases such as $\text{Al}_7\text{Cu}_2\text{Fe}$ and Al_2CuMg to increase in area percentage. Grain boundary melting, triple points, and lamellar phase are also expected to be present at this point and will all increase with elevated temperature and extended hold times. Al_2CuMg , $\text{Al}_7\text{Cu}_2\text{Fe}$, and the lamellar phase should all increase exponentially with increasing temperature and hold times: as the diffusion rate increases it is expected that an increasing amount of phase formation will occur, particularly along the grain boundaries. However, the area percentage of triple-points is expected to increase linearly. As higher temperatures and hold times are reached, grain growth will occur which will limit the amount of grain boundaries. As triple-points are only able to occur along grain boundaries, the growth of this microstructural feature will be limited. The hardness of the AA7075 samples should decrease with increasing temperatures and hold times, due to more strengthening precipitates being put into solution. The nature of this decrease in hardness is expected to be linear: as the temperature of the solution anneal increases, the more effective the solution anneal should be at dissolving any strengthening precipitates. A summary of hypothesized results is shown in Tables 6 and 7.

As for determining what happened to the 'Case A' material, it is hypothesized that it experienced temperatures in excess of 980°F. It is hypothesized that incipient melting will begin to occur at approximately 925°F, but the beginning signs of incipient melting are the agglomeration of Al_2CuMg and the formation of eutectic. The 'Case A' material demonstrates networks of eutectic phase along the grain boundaries paired with triple points, which indicates that it was exposed to much higher temperatures.

Table 5. Hypothesized likelihood of incipient melting occurring based on temperature/time

Temperature	Time		
	1 hr	12 hrs	24 hrs
870°F	Not Likely		
925°F	Likely		
980°F	Extremely Likely		
1035°F	Extremely Likely	Extremely Likely	Extremely Likely
1090°F	Extremely Likely		

Table 6. Hypothesized results for microstructural features and hardness properties

Feature	Expected Trend with Increasing Temp./Hold Time
Al_2CuMg	Increase
Eutectic Phase	Increase
$\text{Al}_7\text{Cu}_2\text{Fe}$	Increase
Triple-Points	Increase
Hardness	Decrease

4. RESULTS

4.1. Optical Microscopy

4.1.1. Temperature-Dependent Data

The temperature-dependent results for optical microscopy are displayed in Figure 4. There were minimal differences between the wrought and 870°F solution anneal conditions. Slightly more agglomeration of the Al_2CuMg phase was evident in the 870°F solution anneal sample, but there were no visual signs of incipient melting in either sample. The voids in both samples are pre-existing from the original wrought condition and were not considered potential triple-points. The 870°F sample image is an example of what a typical sample of AA7075 would look like after a solution anneal adhering to AMS 2770 Rev. P specification [1].

It was at the 925°F solution anneal stage where the beginning signs of agglomeration of the Al_2CuMg became more apparent, especially along grain boundaries. Outside of the increased Al_2CuMg agglomeration, there were no signs of triple-points, cracking, or eutectic phase. The 980°F solution anneal condition showed continued signs of Al_2CuMg agglomeration. The agglomeration remained concentrated along the grain boundaries: a closer look revealed that the agglomeration may be orienting itself primarily at triple-points.

At 1035°F, more distinct signs of incipient melting appeared. Increased agglomeration of Al_2CuMg led to the formation of eutectic phase and rosettes, with higher amounts of eutectic phase located along the grain boundaries. Triple-points were scattered throughout the sample, often adjacent to the eutectic phase. At 1090°F, the same signs of incipient melting were present, but the eutectic phase formed a continuous network along the grain boundaries, interrupted only by triple-points or cracking. Of note in both the 1035°F and 1090°F samples were the increased area percentage of $\text{Al}_7\text{Cu}_2\text{Fe}$. While it is possible that these particles were present in the lower temperature regimes, they were not consistently detected. At both the 1035°F and 1090°F temperatures, these particles were quite enlarged and easily detectable, suggesting that $\text{Al}_7\text{Cu}_2\text{Fe}$ particles thrive at higher temperatures and could perhaps be another indicator of incipient melting.

While obvious signs of incipient melting didn't occur until 1035°F, careful examination of the samples indicated that the process of incipient melting started at approximately 925°F. Comparing these results to 'Case A' in Section 1.2, there are similarities between the 'Case A' material and the 1035°F sample. Both exhibited signs of triple-points and increased agglomeration of Al_2CuMg . However, one significant difference was that the 1035°F sample demonstrated a network of eutectic phase along the grain boundaries, while the 'Case A' material did not. This difference most likely can be attributed to the fact that the 'Case A' material also experienced a forging process, where the strain from forging helped initiate incipient melting at a lower temperature where triple-points formed yet eutectic phase didn't.

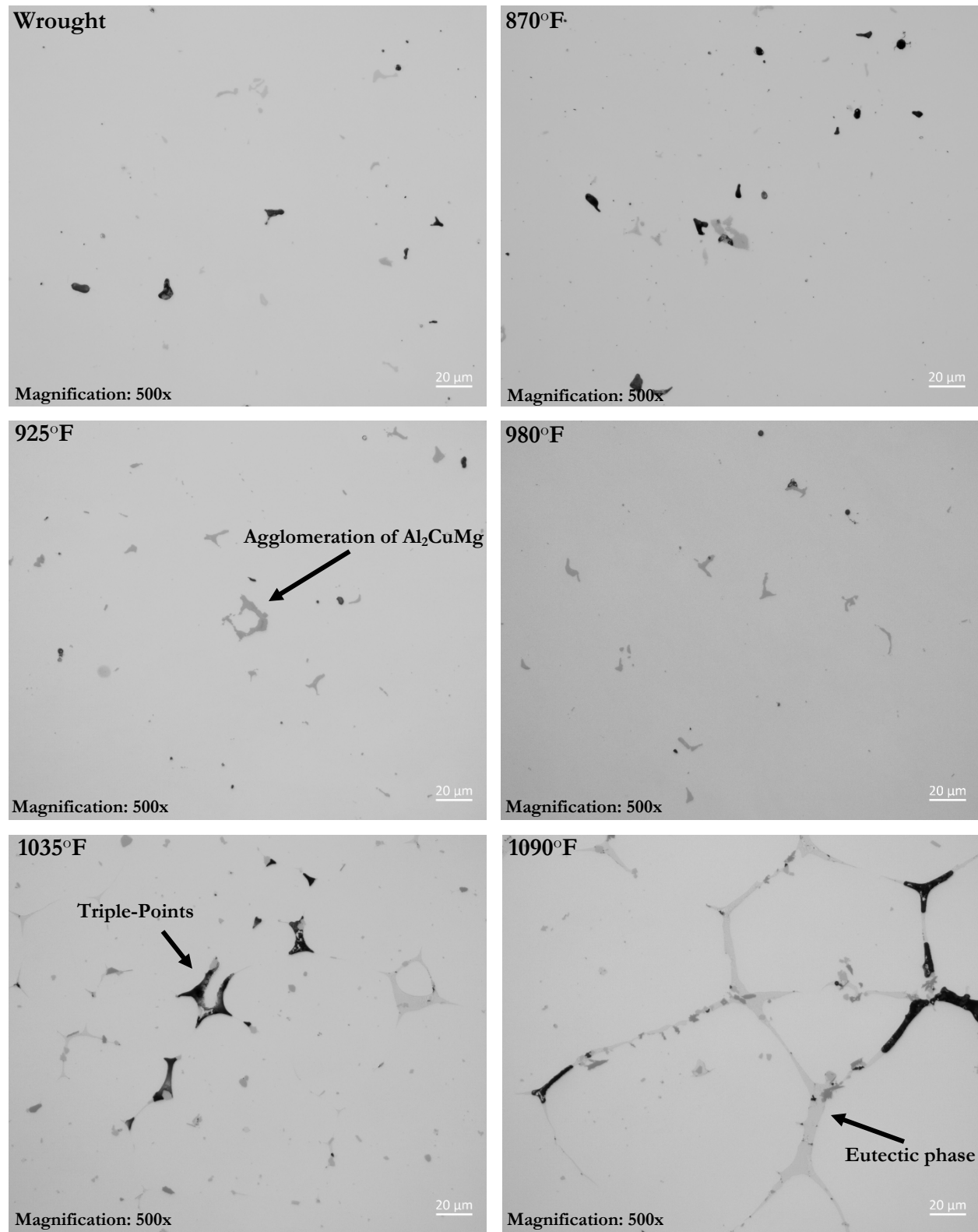


Figure 4. Temperature-dependent micrographs

4.1.2. Time-Dependent Data

The time-dependent results for optical microscopy are displayed in Figure 5. When first analyzing the optical microscopy results for the time-dependent component of the experiment, very little could be differentiated. While the 12-hour and 24-hour samples displayed increased networking of the eutectic phase along the grain boundaries, each of the three samples displayed the same signs of incipient melting (triple points, agglomeration of Al_2CuMg , eutectic phase, rosettes, etc.). However, when viewing the samples at a lower magnification, more discernable differences could be found (Figure 6). It appeared that extended hold times led to increased cracking along the grain boundaries. This was particularly noticeable for the 24-hour hold time sample.

When identifying the amount of time an AA7075 sample has seen at an elevated temperature, examining the extent of cracking at a lower magnification may help. Comparing these results to 'Case A', it could be assumed that the material didn't experience a high temperature for an extended period of time. There are isolated triple-points, but there are no large networks of cracks that are extending along grain boundaries, nor are there networks of eutectic phase. The data suggests that the 'Case A' material was heat treated for a time that adhered to AMS 2770 Rev. P [1].

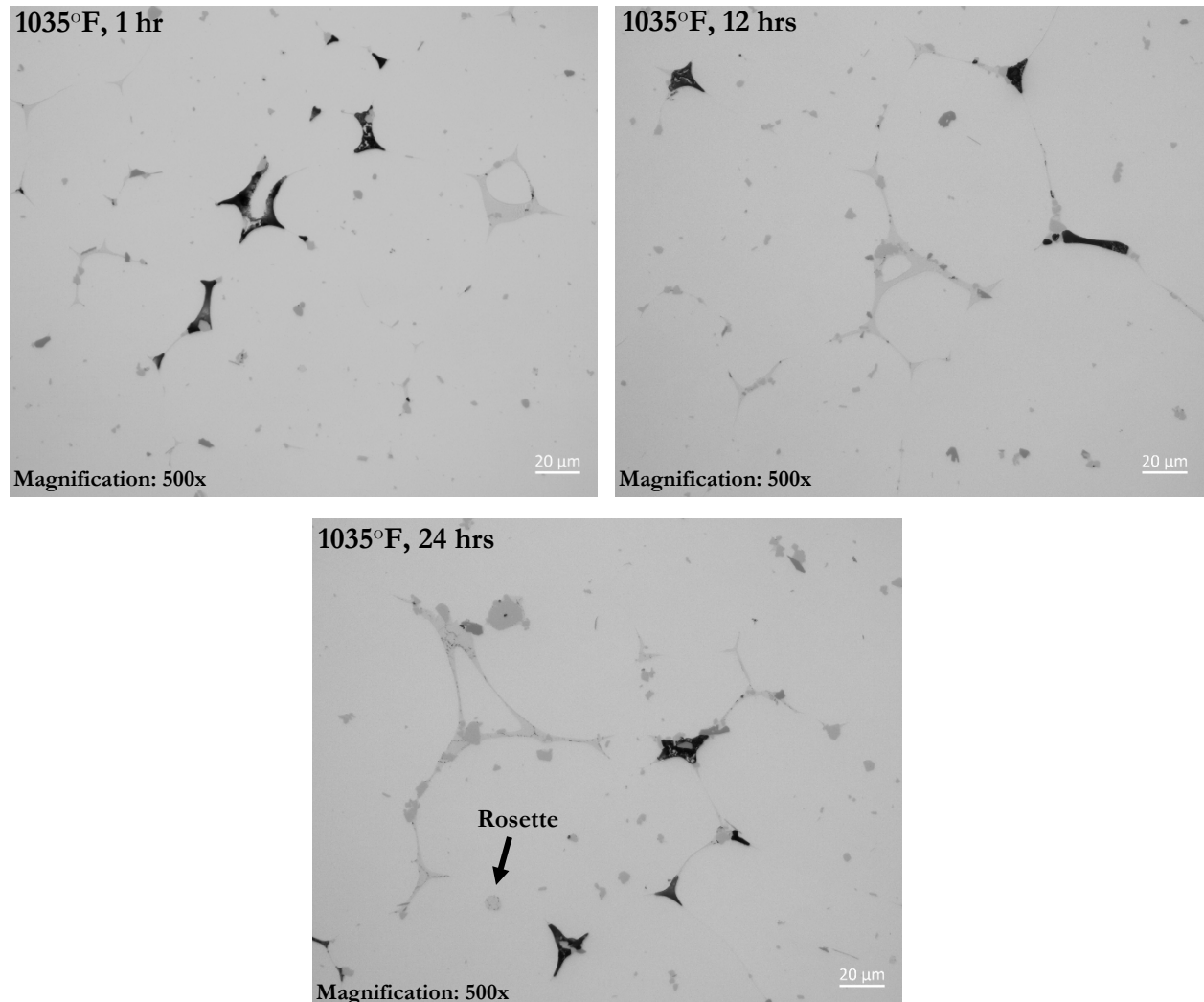
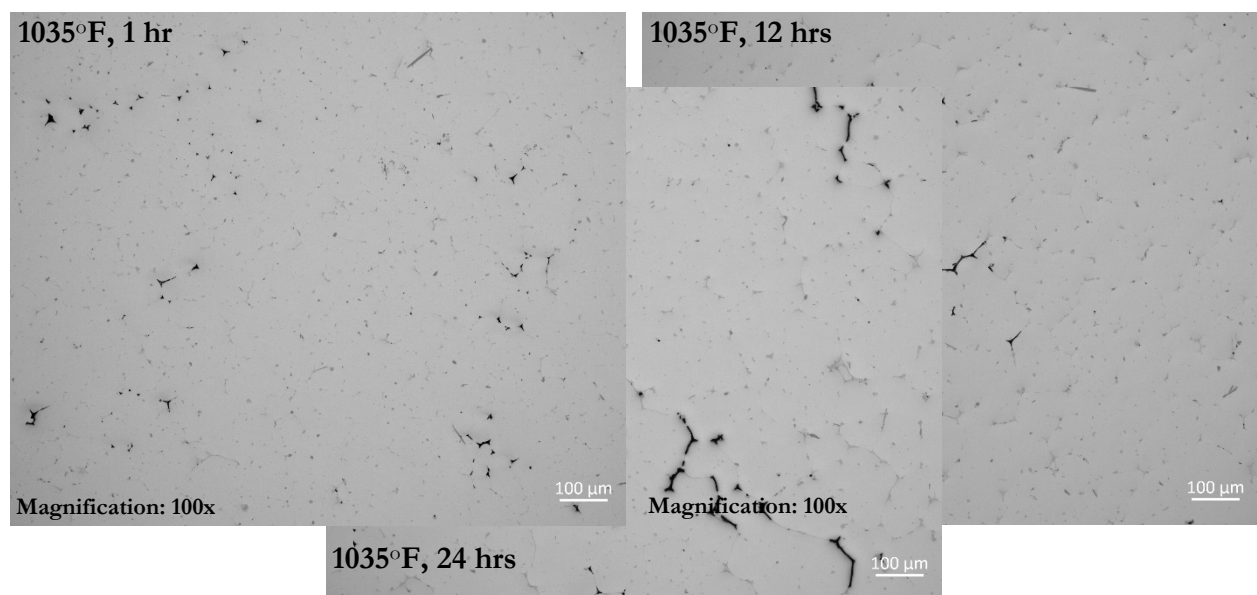


Figure 5. Time-dependent micrographs



Magnification: 100x

Figure 6. Extent of cracking in time-dependent samples

4.2. Electron Dispersive Spectroscopy

To better determine the phases and their evolution in relation to temperature and hold time, electron dispersive spectroscopy was used to help qualitatively identify some phases. Looking at the optical image in Figure 7, one of the most noticeable aspects was the large needle-like structure located along the lamellar phase. The EDS mapping results indicate that this structure was concentrated in aluminum and iron and deficient in magnesium. Based on literature review of the microstructural phases commonly present in AA7075, this needle-like structure most likely is $\text{Al}_7\text{Cu}_2\text{Fe}$ [3,4]. When further comparing both the EDS map and the optical image in Figure 7, the $\text{Al}_7\text{Cu}_2\text{Fe}$ was a darker grey phase that appeared both as a needle and as a blocky constituent.

The interconnected phase present along the grain boundaries is another feature of Figure 7. When viewing this structure using optical microscopy, it appeared as a light grey phase with a lamellar-like structure. Using the EDS mapping results, it appeared as though this phase is alloy-rich with high concentrations of magnesium, zinc, copper and low concentrations of aluminum, iron,

and chromium. This phase was most likely the eutectic phase that forms adjacent to the Al_2CuMg particles as agglomeration occurs. As the Al_2CuMg agglomerates, it starts to pull MgZn_2 out of solution, leaving behind a low melting eutectic that is depleted of aluminum. The fact that this eutectic phase formed a network along the grain boundaries speaks to the extent of incipient melting that occurred.

Sprinkled throughout the optical image in Figure 7 are blocky grey particles. These particles were lighter in color than the $\text{Al}_7\text{Cu}_2\text{Fe}$ yet darker in color than the eutectic phase. Based on EDS mapping, these particles are high in aluminum, chromium, and magnesium. Literature review would suggest that this type of particle is Al_2CuMg [3,4]. This would align with the fact that Al_2CuMg often were surrounded by eutectic phase and were found to be agglomerating at lower temperatures. However, the high amounts of chromium and low amounts of copper in these particles still don't match up with the composition of Al_2CuMg . The EDS mapping suggests that chromium could be replacing the copper and an aluminum-chromium-magnesium particle could be serving the same role as the Al_2CuMg , but more research is needed to definitively determine if this is true. For the purposes of this report and to stay consistent with literature data, these particles were referred to as Al_2CuMg .

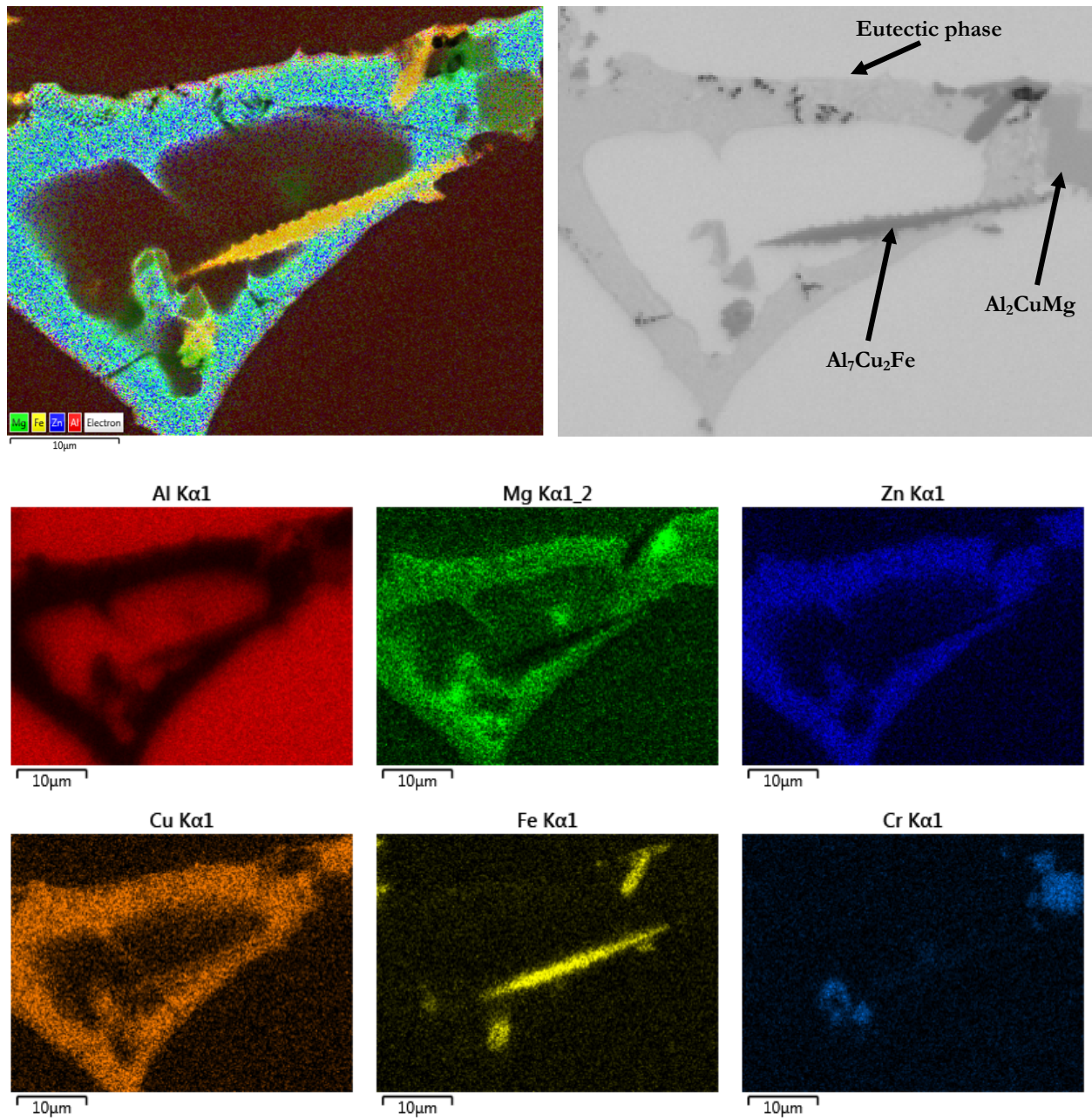


Figure 7. EDS map of 1090°F sample

4.3. Zeiss Intellesis Image Analysis

The Zeiss Intellesis image analysis software produced valuable data and showed promise for future microstructural analysis. Both the temperature-dependent and time-dependent data showed interesting trends with the microstructural constituents, listed in Tables 7 and 8. While only one randomly selected 500x magnification image was used per temperature condition due to time constraints, the data was consistent with observations from optical microscopy. Further iterations of Zeiss Intellesis image analysis using more temperature and hold time conditions as well as sampling larger surface areas are recommended for future investigation.

Zeiss Intellesis image analysis software utilizes machine-learning to recognize microstructures. Once an image is uploaded, microstructural phenomena can be manually shaded in to guide the software on how to execute characterization. Once several iterations of shading by the user have been performed, a template can be created and applied to other images with similar microstructures. Unfortunately, due to the fact that the software takes manual shading and then characterizes a micrograph based on this shading, error cannot easily be calculated for measurements. There is error associated with each measurement, but that is dependent upon the user's shading accuracy along with the software's ability to apply the shading to an entire micrograph. For this experiment, a qualitative check was performed after each image analysis iteration to clarify that the software was working and the phenomena were being shaded in correctly. Additionally, a 50% confidence level setting was used when performing the image analysis. This confidence level setting was the highest confidence setting that could be used without the software 'greying' out regions and not including these regions in the final image analysis.

4.3.1. Temperature-Dependent Data

There was a clear positive correlation between temperature and eutectic phase. This relationship was expected, given that higher temperatures allow for the eutectic to further develop and grow. Visually, Figure 9 demonstrates this relationship. The eutectic phase was colored purple by the Intellesis software, and as the temperature increased, it became apparent that there was a larger area percentage of purple. There was also clear positive correlation between temperature and triple-points. Triple-points were colored green by the Intellesis software, and as the temperature increased, it became obvious that there was a larger area percentage of green.

Both the Al₂CuMg and Al₇Cu₂Fe data were inconclusive. Perhaps increasing the surface area scanned and using more iterations of Zeiss Intellesis would yield clearer results, but the current body of data does not suggest there is any clear relationship between temperature and either of these phases.

Table 7. Zeiss Intellesis image analysis results for temperature-dependence

Temperature	Microstructural Constituents				
		Al ₂ CuMg	Al ₇ Cu ₂ Fe	Eutectic Phase	Triple-Points
980°F	0.718%	Not Present	Not Present	Not Present	Not Present
1035°F	1.000%	0.517%	1.315%	0.252%	
1090°F	0.628%	0.380%	3.819%	0.867%	

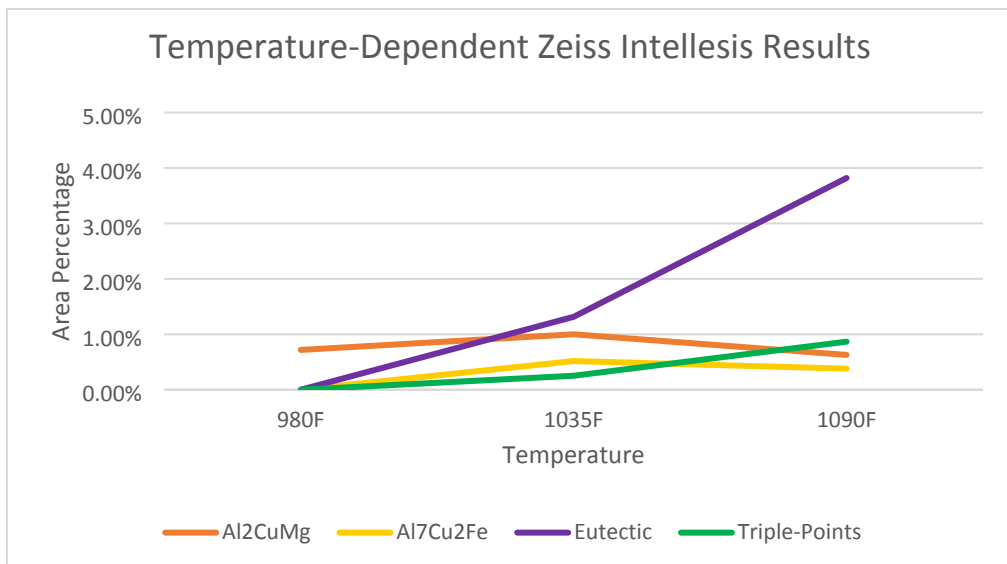


Figure 8. Trends in the Zeiss Intellesis data for temperature-dependence

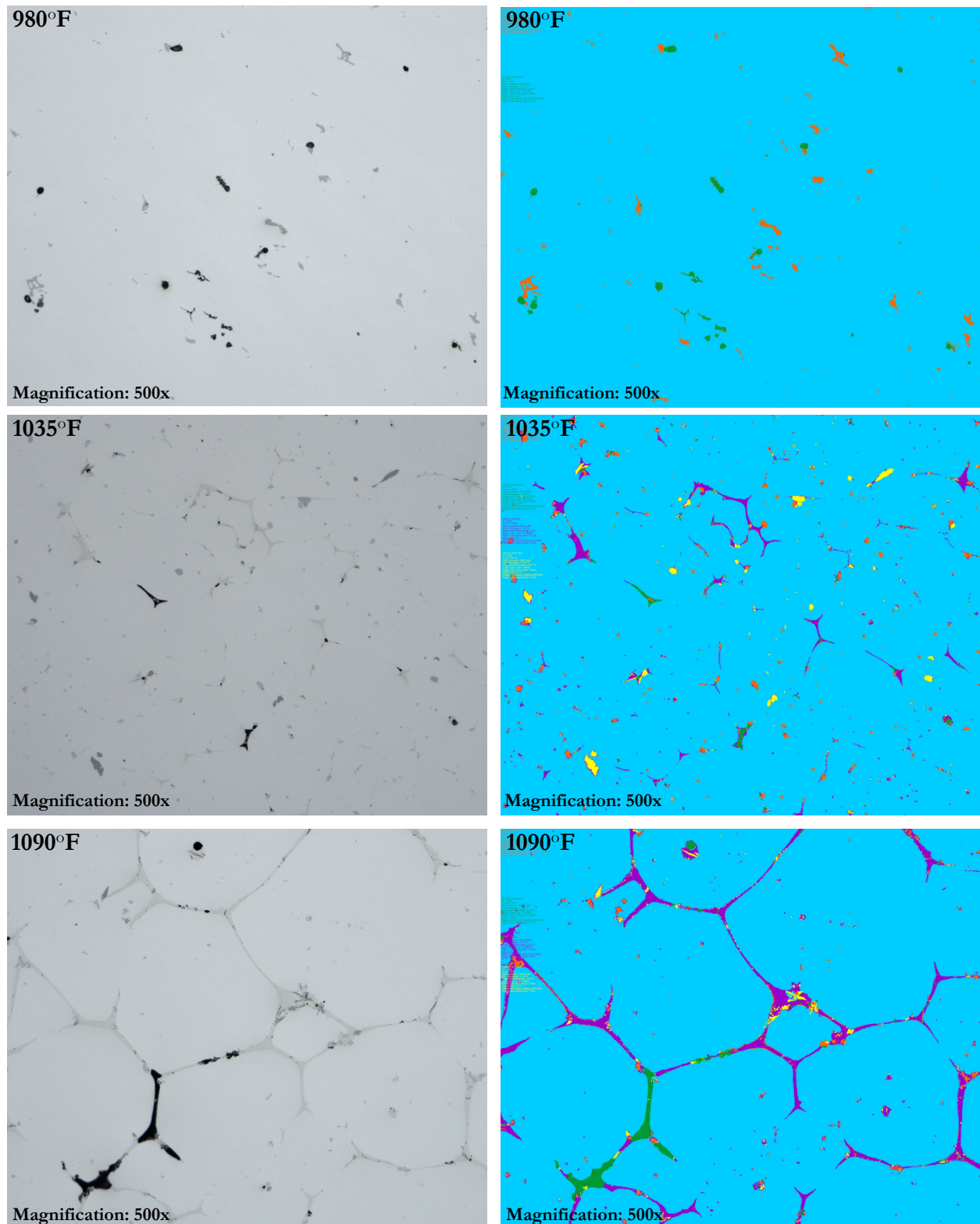


Figure 9. Temperature-dependent Zeiss Intellesis image analysis results

4.3.2. Time-Dependent Data

The time-dependent data demonstrated similar trends to the temperature-dependent data. Both the Al_2CuMg and $\text{Al}_7\text{Cu}_2\text{Fe}$ data showed that the area percentage of each phase stays relatively stable as the hold time changes. This indicated that hold time does not impact the area percentage of either of these phases.

The eutectic phase data did not yield any clear results. The 12-hour hold time condition had a lower area percentage of eutectic phase than the 1-hour hold time condition, which was not expected. One reason that this may have occurred is simply because not enough surface area was sampled, and the lower area percentage of eutectic for the 12-hour hold time isn't representative. Performing analysis on more images would correct this problem. Another potential reason is that hold time may not be an integral variable into the amount of eutectic present in a sample, and the area percentage of eutectic remained stable.

There was a positive correlation between triple-points and hold time. This agreed with the results from Section 4.1, where it was observed that the best way to tell the difference between samples with different hold times is to observe the amount of cracking present in the sample.

Table 8. Zeiss Intellesis image analysis results for time-dependence

Hold Time	Microstructural Constituents			
	Al_2CuMg	$\text{Al}_7\text{Cu}_2\text{Fe}$	Eutectic Phase	Triple-Points
1 hour	1.000%	0.517%	1.315%	0.252%
12 hours	0.856%	0.281%	1.168%	0.328%
24 hours	1.005%	0.335%	1.440%	0.817%

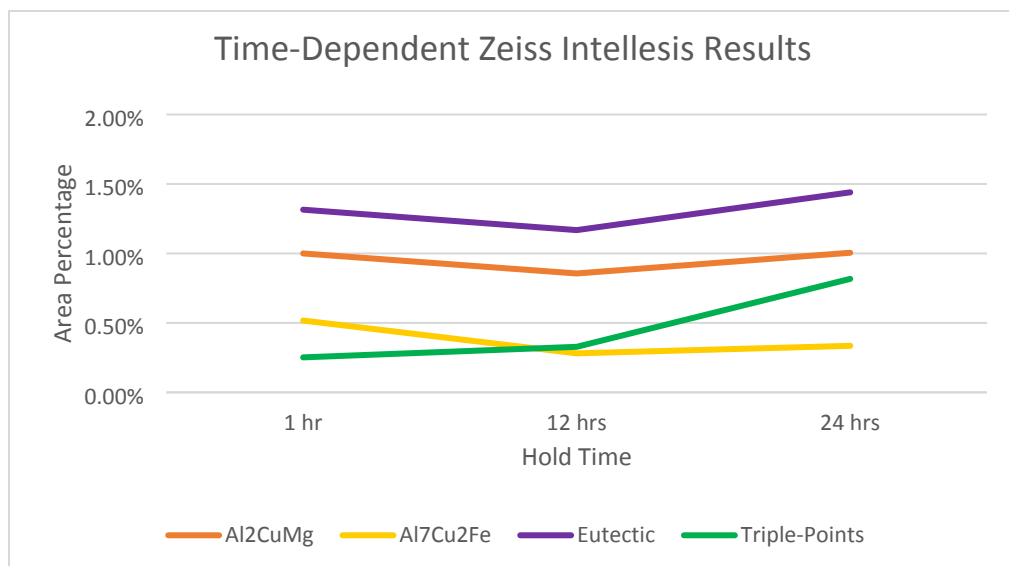


Figure 10. Trends in the Zeiss Intellesis data for time-dependence

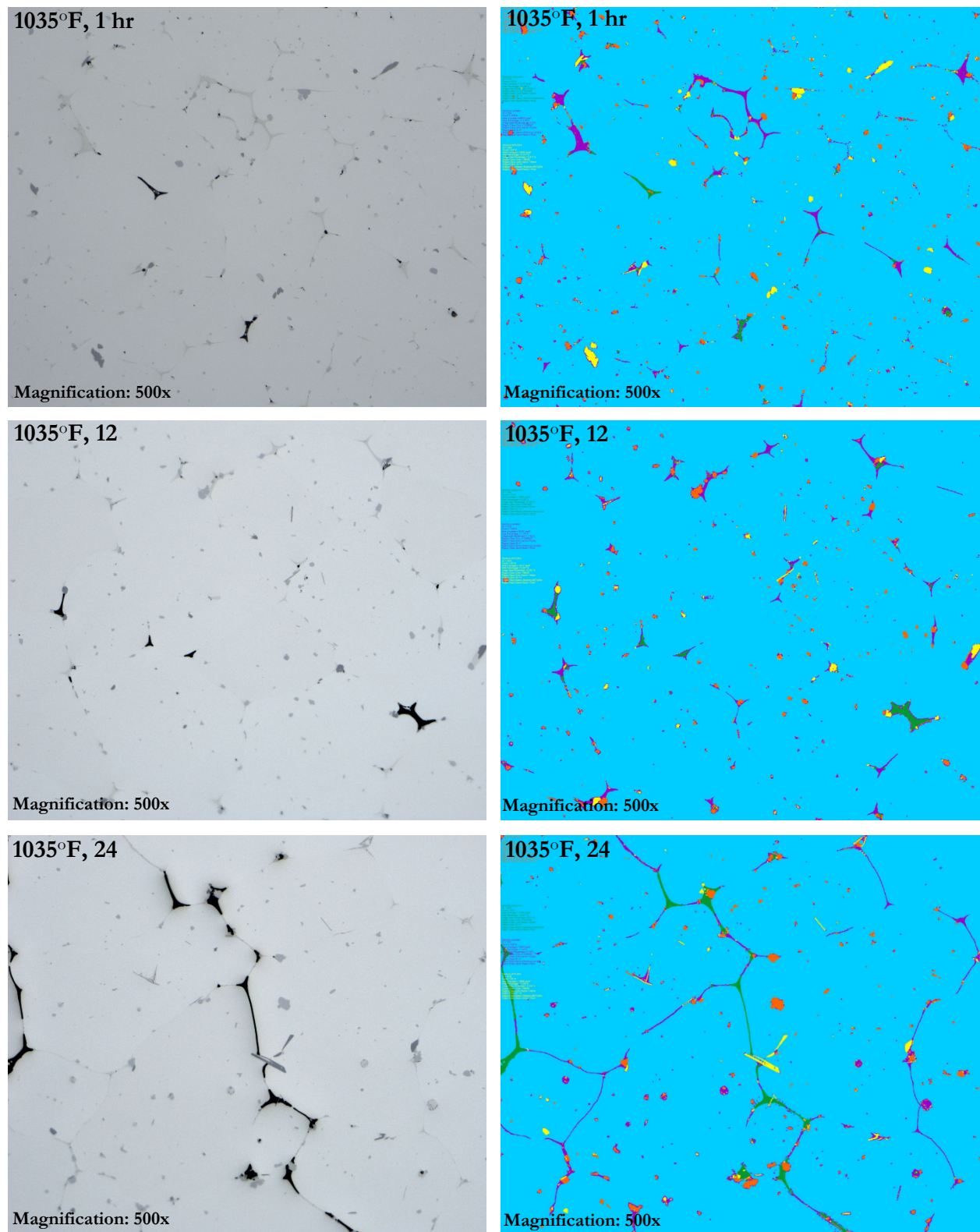


Figure 11. Time-dependent Zeiss Intellesis image analysis results

4.4. Vickers Micro-Indentation

4.4.1. Temperature-Dependent Data

The temperature-dependent component (Fig. 13) of the experiment yielded mostly expected results. The as-received AA7075 sample exhibited the highest hardness while the 1090°F solution anneal sample had the lowest hardness. However, between 870°F – 980°F, the hardness remained consistent and did not drop with temperature. This indicated that the primary microstructural evolution of Al₂CuMg agglomeration does not impact the bulk hardness of the sample. At 1035°F and above, there was a more pronounced decrease in hardness which corresponds to large-scale incipient melting. At 1035°F, triple-points were observed, and eutectic phase accumulated along the grain boundaries. At 1090°F, there was an even larger drop in hardness with corresponding increase in area fraction of triple points and cracking within the samples.

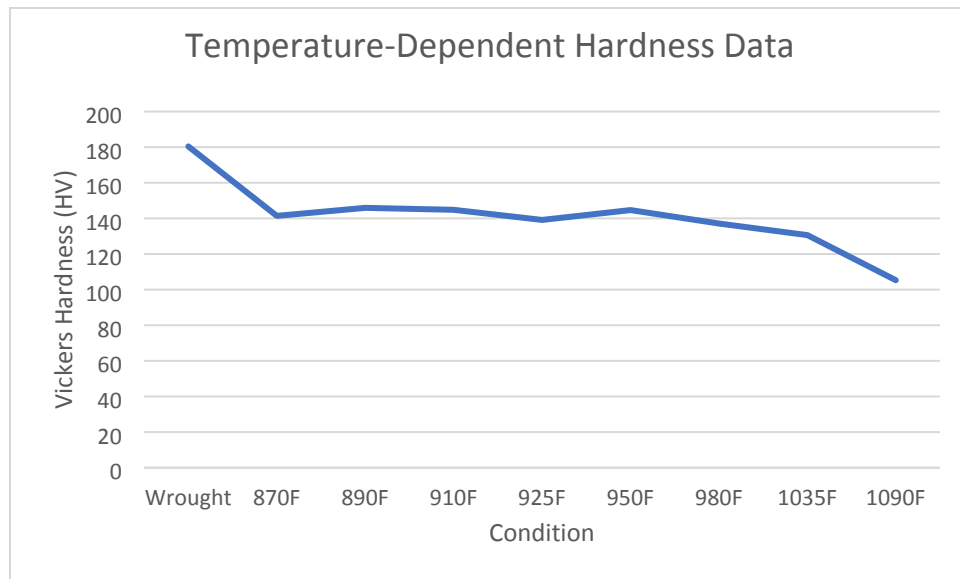


Figure 12. Temperature-dependent hardness data

4.4.2. Time-Dependent Data

The time-dependent component (Fig. 14) of the experiment yielded surprising hardness results. Although the extent of cracking throughout the samples drastically increased with increasing time (per Section 4.1), the average hardness of the samples did not show a corresponding decrease.

When examining both the temperature and time-dependent components of the experiment, the results suggested that temperature plays the most impactful role in determining the hardness of a sample. However, even the temperature-dependent component of the study didn't exhibit large differences in hardness until well after signs of incipient melting were determined in the microstructure. Based on this data, hardness testing is not as trustworthy as optical microscopy when determining whether incipient melting has occurred in AA7075.

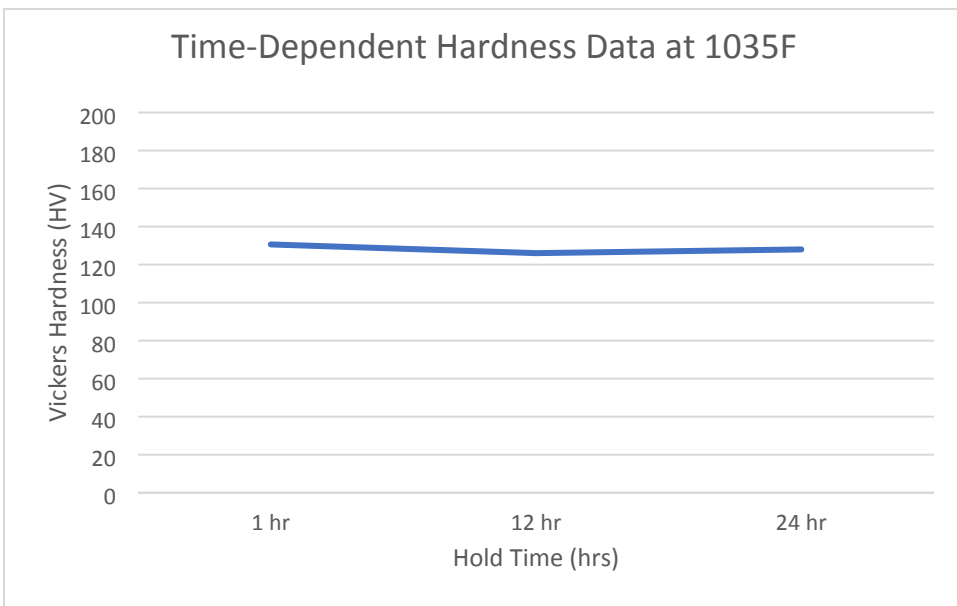


Figure 13. Time-dependent hardness data

REFERENCES

- [1] SAE International, “Aerospace Material Specification: Heat Treatment of Wrought Aluminum Alloy Parts AMS 2770 Rev. P.” Warrendale, PA, Apr-2019.
- [2] ASTM International, “Standard Specification for Aluminum and Aluminum-Extruded Bars, Rods, Wire, Profiles, and Tubes.” West Conshohocken, PA, 11-June-2020.
- [3] J. E. Hatch, Ed., *Aluminum: Properties and Physical Metallurgy*. Metals Park, Ohio: American Society for Metals, 1984.
- [4] T. Kilkenny, “Digital Commons - Cal Poly,” An Investigation of Incipient Melting During Solution Heat Treatment of 7050 Aluminum Forgings and Its Effect on Corrosion Properties. [Online]. Available: <https://digitalcommons.calpoly.edu/cgi/viewcontent.cgi?article=1127&context=matesp>. [Accessed: 31-May-2022].
- [5] A N Aliyah and A Anawati 2019 IOP Conf. Ser.: Mater. Sci. Eng. 541 012007
- [6] Okamoto, “Aluminum Zinc Binary Phase Diagram,” *Alloy Phase Diagram Database*, ASM International, 1995.

DISTRIBUTION

Email—Internal

Name	Org.	Sandia Email Address
Technical Library	1911	sanddocs@sandia.gov

This page left blank



**Sandia
National
Laboratories**

Sandia National Laboratories is a multimission laboratory managed and operated by National Technology & Engineering Solutions of Sandia LLC, a wholly owned subsidiary of Honeywell International Inc. for the U.S. Department of Energy's National Nuclear Security Administration under contract DE-NA0003525.